DOI: 10.28919/ejma.2022.2.7

Eur. J. Math. Appl. (2022)2:7
URL: http://ejma.euap.org

CONTROL DESIGN FOR BILATERAL TELEOPERATION SYSTEM WITH ACTUATOR DEAD-ZONE AND TIME-VARYING DELAYS

AWATEF K. ALI[1] AND MAGDI S. MAHMOUD[2,*]

Abstract. This paper investigates the control design of a bilateral teleoperation system with input dead-zone, dynamic uncertainties, external disturbances and time-varying delay. Our objective is to achieve a robust bilateral teleoperation with guaranteed position asymptotic convergence. This is accomplished using an efficient backstepping approach combined with nonsingular fast terminal sliding mode control (NFTSMC) where the uncertain dynamics of the system are identified using radial basis function neural network (RBFNN). The upper-bounds of the external disturbances together with the RBFNN approximation errors are estimated and compensated online using adaptation algorithms. Computer simulations are provided to demonstrate the viability of the proposed control law.

1. Introduction

The applications of teleoperation are ever growing and expanding in many areas, such as industries, hazardous environments, medical, space exploration, undersea exploration and robotic construction [1], [2], [3], [4]. By and large, teleoperation is mainly categorized into:

- Unilateral and
- Bilateral.

The former sends only the force signal via communication channel to the slave plant, while the later transmits force information from the master to slave and from the slave to the master. A bilateral teleoperation system comprises of the human operator, master, slave, environment and the communication channel [5], [6]. The presence of time-delay in the communication channel deteriorate the stability and subsequently the performance of the system [7], [8]. In addition, the existence of modeling uncertainties, unknown loads, and external disturbances further degrade the performance of the system.

In this regards, the control problem of bilateral teleoperation has essentially drawn an enormous interest over the past years and several control methods were designed for both theoretical and practical applications. A guaranteed performance control of a telerobotic has been achieved

[1]Electronics Department, National Institute of Telecommunications, Nasr City, Cairo-Egypt

[2]Control and Instrumentation Engineering Department, KFUPM, P. O. 5067, Dhahran 31261, Saudi Arabia

*Corresponding author

E-mail addresses: 3watef@gmail.com, msmahmoud@kfupm.edu.sa.

Key words and phrases. bilateral teleoperation; dead-zone; radial basis function neural network (RBFNN); nonsingular fast terminal sliding mode control (NTSMC); backstepping.

Received 30/01/2022.

at both dynamic and kinematic levels [9]. A NTSMC for a force sensor-less bilateral teleoperation system has been developed in [10]. In [11], the trajectory tracking accuracy of bilateral teleoperation has been enhance by integrating support vector machine with variable gain control. An adaptive control of telerobotic system with dynamic uncertainties was utilized in [12]. An output feedback control of bilateral teleoperation system with state constraints has been proposed in [13]. A tele-operated control of bilateral hydraulic system is achieved using SMC with sliding mode perturbation observer [14]. A force sensor-less control of bilateral dissimilar master-slave system has been presented in [15]. Despite the fact that the foregoing methods can ensure both transient and steady state performances, the impact of time delays were not considered. The effects of constant time delays in teleoperation systems has been dealt with using nonlinear disturbance observer based control [16], [17], a bilateral impedance control [18], event-triggered adaptive bilateral control [19], output feedback synchronization control [20], fault-tolerant control [21], adaptive neural network control [22], an integral SMC optimized with particle swamp optimization [23], an adaptive NTSMC [24]. However, due to the uncertainties associated with teleoperation system, the time delays cannot be constant. Several control architectures were introduced to handle tracking problems in bilateral teleoperation system with time-varying delays, such as robust adaptive type-2 fuzzy control [25], adaptive type-2 fuzzy neural-network control [26], linear matrix inequalities control [27], internet-based control [28], neural-network based control [29], composite adaptive control [30], adaptive finite time control [31], task space control [32], adaptive fuzzy backstepping control [33], robust adaptive control [34], RBFNN-based SMC [35], dynamic gain control [36], adaptive fault tolerant control [37].

Non-smooth nonlinearities (i.e. backlash, dead zone, hysteresis & saturation) appear in the actuator of many systems such as power systems, robotic systems, chemical processes and so on. These nonlinearities severely deteriorate system performance, give rise to poor transient response, and system instability [38]. To deal with the actuator nonlinearities, many investigators have suggested diverse control techniques. In [39], a force feedback control with sliding mode observer has been studied for a bilateral teleoperation with unknown Prandtl-Ishlinskii hysteresis. In [40], synchronization control problem of bilateral teleoperation plant with Backlash-Like hysteresis has been presented. In [41], a position tracking controller for teleoperation system with input deadzone was proposed. The control schemes tackling actuator saturation in teleoperation systems are presented in [42], [43], [44], [45], [46], [47], [48], [49].

It is worth noting that the control of teleoperation system with actuator dead-zone is reported for the first time in [41] and has not been considered afterward. However, the authors considered the effect of the dead-zone in the slave side only. In addition, the inevitable time delay in the communication channel was not addressed. Therefore, a good control formulation to handle the aforesaid issues concurrently is challenging.

In this paper, we build on the published work [24]- [41] and extend them further to develop an improved control scheme for a bilateral teleoperation system with dynamic uncertainties, external disturbances, time-varying delay and input dead-zone. The contributions of the paper are summarized by the following points:

- We provide a new control design method to effectively handle both the time-varying delay and the dead-zone nonlinearities in the master-slave actuators.

- A backstepping method is combined with nonsingular fast terminal sliding mode control (BNFTSMC) for upgraded transparency and guaranteed stability of the bilateral teleoperation system.
- A radial basis function neural network (RBFNN) is employed to identify the uncertain dynamics of the system. The upper-bounds of the RBFNN approximation errors and the external disturbances are updated online.
- No prior information about the system dynamics and external disturbances is needed. The closed-loop system has been shown to converge to a small neighborhood of the origin using Lyapunov stability analysis.

This work is structured as: Section 2 describes the nonlinear model and some properties of the teleoperation system. Section 3 presents the control design. Section 4 gives the results and discussions. Section 5 provides the conclusions.

2. Problem Presentation

This section presents the nonlinear dynamic model and some properties of the teleoperation systems. The Euler-Lagrange equations describing the dynamics of the teleoperation plant are [30]

$$\begin{aligned} P_m(q_m)\ddot{q}_m + Q_m(q_m,\dot{q}_m)\dot{q}_m + G_m(q_m) + \Delta_m \\ = D_m(\tau_m) + \tau_h \end{aligned} \tag{1}$$

$$P_s(q_s)\ddot{q}_s + Q_s(q_s,\dot{q}_s)\dot{q}_s + G_s(q_s) + \Delta_s = D_s(\tau_s) + \tau_e \tag{2}$$

where $P_i \in \mathcal{R}^{n\times n}, Q_i \in \mathcal{R}^n, G_i \in \mathcal{R}^n, i = m,s$ stand for the inertia matrix, Coriolis's and centrifugal terms vector, and the gravity vector respectively; $D_i(\tau_i) \in \mathcal{R}^n, i = m,s$ are the deadzone outputs; $\tau_i \in \mathcal{R}^n, i = m,s$ are the control inputs; $\tau_h, \tau_e \in \mathcal{R}^n$ are the human and the environmental contact forces; $\Delta_i \in \mathcal{R}^n, i = m,s$ represent the external disturbances and the modelling error. The equations of motion of the master and slave systems satisfy the following properties [33]:

Property 1: The matrix $\left[\dot{P}_i(q_i) - 2Q_i(q_i,\dot{q}_i)\right] > 0$ is skew symmetric.

Property 2: $P_i(q_i) = P_i^T(q_i) > 0, b_1 I \le P_i(q_i) \le b_2 I, i = m,s,$ with b_1 and b_2 are scalars.

Property 3: The model can be transformed to a linear parameterized model as

$$P_i(q_i)\ddot{q}_i + Q_i(q_i,\dot{q}_i)\dot{q}_i + G_i(q_i) = R_i(q_i,\dot{q}_i,\ddot{q}_i)\vartheta_i \tag{3}$$

where $R_i(q_i,\dot{q}_i,\ddot{q}_i)$ represent the regressor matrices, and ϑ_i denote the vectors of parameters.

Assumption 1: The external disturbances and the RBFNN approximation errors (ϵ_i) are bounded by

$$\Delta_i + \epsilon_i \le \alpha_{i0} + \alpha_{i1}|e_i| + \alpha_{i2}|\dot{e}_i| \quad (i = m,s) \tag{4}$$

where α_{i0}, α_{i1} and α_{i2} are unknown constants.

The deadzone model is expressed as [50]

$$D_i(\tau_i) = \begin{cases} [\tau_i - \pi_{\mathrm{ri}}(t)], & \tau_i \ge \pi_{\mathrm{ri}}(t), \\ 0, & -\pi_{\mathrm{li}}(t) < \tau_i < \pi_{\mathrm{ri}}(t) \\ [\tau_i + \pi_{\mathrm{li}}(t)], & \tau_i \le -\pi_{\mathrm{li}}(t), i = m,s \end{cases}$$

where $\pi_{\mathrm{ri}}(t)$ and $\pi_{\mathrm{li}}(t)$ are the unknown time-varying deadzone parameters. The τ_i can be written as

$$D_i = \tau_i + \Pi_i < i = m, s \tag{5}$$

$$\text{Where } \Pi_i = \begin{cases} -\pi_{\mathrm{ri}}(t) & \tau_i \geq \pi_{\mathrm{ri}}(t) \\ -\tau_i & -\pi_{\mathrm{li}}(t) < \tau_i < \pi_{\mathrm{ri}}(t) \\ \pi_{\mathrm{li}}(t) & \tau_i \leq -\pi_{\mathrm{li}}(t),\ i = m, s \end{cases}$$

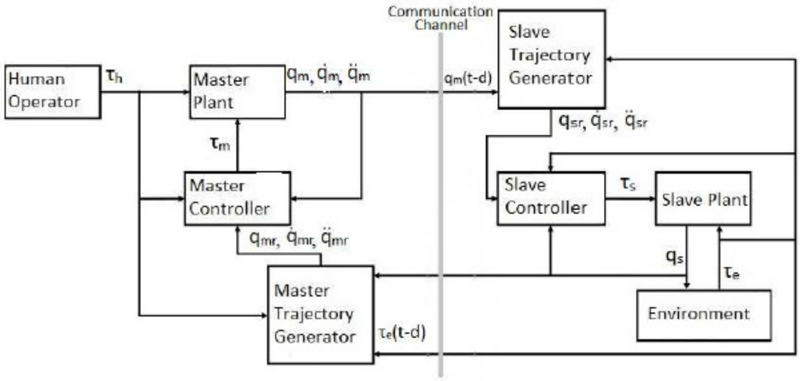

FIGURE 1. Proposed bilateral teleoperation control scheme

3. CONTROL OF THE NONLINEAR TELEOPERATION SYSTEM

In this section, the BNFTSMC-RBFNN is designed for both the master and the slave subsystems. The schematic diagram of the overall control system is shown in Fig. 1.

3.1. RBFNN definition.

Due to the prominent properties of RBFNN algorithms in function approximations, the RBFNN is widely used in nonlinear control and systems modelling. The RBFNN can approximate any continuous function $\Theta : \mathcal{R}^j \longrightarrow \mathcal{R}$ over a compact domain $\Upsilon \in \mathcal{R}^j$ given by

$$\Theta(x) = W^T \Psi(x) + \epsilon \; \forall x \subset \Upsilon \in \mathcal{R}^j \tag{6}$$

where $x \subset \Upsilon \in \mathcal{R}^j$ is the input vector, $W \in \mathcal{R}^{d\times 1}$ is the RBFNN weight vector, $\epsilon > 0$ is the bounded RBFNN approximation error, $\Psi = [\Psi_1, \Psi_2, \dots, \Psi_d]^T \in \mathcal{R}^{d\times 1}$ is a Gaussian function vector defined as

$$\Psi_i = exp\frac{-(x-c_i)^T(x-c_i)}{v^2} \tag{7}$$

where $c_i \in \Upsilon$ and $v > 0$ denote the center and the width of the Gaussian function respectively.

3.2. Slave control design.

The reference slave signals $q_{\mathrm{sr}}(t), \dot{q}_{sr}(t), \ddot{q}_{sr}(t)$ can be obtained by passing the delayed master position $q_m\left(t - d_(t)\right)$ through the filter $E_f(s) = 1/\left(1 + \tau_f s\right)^2$ [35]. The tracking error can be defined as

$$\begin{cases} e_s = q_{\mathrm{sr}} - q_s \\ \dot{e}_s = \dot{q}_{sr} - \dot{q}_s \\ \ddot{e}_{ss} = \ddot{q}_{sr} + P_s^{-1}\left[Q_s\dot{q}_s + G_s + D_s - \Pi_s - \tau_s - \tau_e\right] \end{cases} \tag{8}$$

Define the NFTSMC manifold as [51]

$$\xi_s = \dot{e}_s + \Lambda_s e_s + \lambda_s \beta_s\left(e_s\right) \tag{9}$$

with $\beta_s\left(e_s\right)$ and its first time-derivative $\dot{\beta}_s\left(e_s\right)$ defined as

$$\beta_s\left(e_{\mathrm{si}}\right) = \begin{cases} \mathrm{sig}\left(e_{\mathrm{si}}\right)^{\sigma_{\mathrm{si}}}, \bar{\xi}_{\mathrm{si}} = 0 \text{ or } \left(\bar{\xi}_{\mathrm{si}} \neq 0, |e_{\mathrm{si}}| > \varepsilon\right) \\ \rho_{\mathrm{si}} e_{\mathrm{si}} + \eta_{\mathrm{si}} sig\left(e_{\mathrm{si}}\right)^{\omega_{\mathrm{si}}}, \bar{\xi}_{\mathrm{si}} \neq 0, |e_{\mathrm{si}}| \leq \varepsilon \end{cases}$$

$$\dot{\beta}_s(e_{\mathrm{si}}) = \begin{cases} \sigma_{\mathrm{si}} |e_{\mathrm{si}}|^{|\sigma_{\mathrm{si}}-1} \dot{e}_{\mathrm{si}}, \bar{\xi}_{\mathrm{si}} = 0 \text{ or } (\bar{\xi}_{\mathrm{si}} \neq 0, |e_{\mathrm{si}}| > \varepsilon_i) \\ \rho_{\mathrm{si}}\dot{e}_{\mathrm{si}} + \eta_{\mathrm{si}}\omega_{\mathrm{si}} |e_{\mathrm{si}}|^{\omega_{\mathrm{si}}-1} \dot{e}_{\mathrm{si}}, \bar{\xi}_{\mathrm{si}} \neq 0, |e_{\mathrm{si}}| \leq \varepsilon \\ i = 1, 2 \ldots, n \end{cases} \tag{10}$$

where $\bar{\xi}_{\mathrm{si}} = \dot{e}_{\mathrm{si}} + \Lambda_{\mathrm{si}} e_{\mathrm{si}} + \lambda_{\mathrm{si}} \beta_{\mathrm{si}}(e_{\mathrm{si}}), 0 < \sigma_{\mathrm{si}} < 1, 1 < \omega_{\mathrm{si}} < 2, \varepsilon > 0$, and ρ_{si} and η_{si} meet the following conditions

$$\rho_{\mathrm{si}} = [(\omega_{\mathrm{si}} - \sigma_{\mathrm{si}}) / (\omega_{\mathrm{si}} - 1)] \varepsilon^{\sigma_{\mathrm{si}}-1}$$
$$\eta_{\mathrm{si}} = [(\sigma_{\mathrm{si}} - 1) / (\omega_{\mathrm{si}} - 1)] \varepsilon^{\sigma_{\mathrm{si}}-\omega_{\mathrm{si}}}$$

Define the Lyapunov function V_{s1} as

$$V_{s1} = \frac{1}{2} e_s^T e_s \tag{11}$$

The time-derivative of V_{s1} can be computed as

$$\dot{V}_{s1} = e_s^T [\dot{q}_{\mathrm{sr}} - \dot{q}_s] \tag{12}$$

The virtual controller is thus

$$\dot{q}_s = -\xi_s + \dot{q}_{sr} + C_s e_s \tag{13}$$

Substituting the controller (13) into (12) yields

$$\dot{V}_{s1} = -e_s^T C_s e_s + e_s^T \xi_s \tag{14}$$

Then, consider the Lyapunov function

$$V_{s2} = \frac{1}{2} e_s^T e_s + \frac{1}{2} \xi_s^T P_s \xi_s \tag{15}$$

The derivative of V_{s2} can be obtained as

$$\begin{aligned} \dot{V}_{s2} &= -e_s^T C_s e_s + e_s^T \xi_s + \tfrac{1}{2} \xi_s^T \dot{P}_s \xi_s + \dot{\xi}_s^T P_s \xi_s \\ &= -e_s^T C_s e_s + e_s^T \xi_s + \tfrac{1}{2} \xi_s^T \dot{P}_s \xi_s \\ &\quad + \xi_s^T [Q_s \dot{q}_s + G_s + \Delta_s + \zeta_s - \Pi_s - \tau_s - \tau_e] \\ &= -e_s^T C_s e_s + \tfrac{1}{2} \xi_s^T \left[\dot{P}_s - 2Q_s\right] \xi_s + \xi_s^T [e_s + Q_s \xi_s \\ &\quad + Q_s \dot{q}_s + G_s + \Delta_s + \zeta_s - \Pi_s - \tau_s - \tau_e] \\ &= -e_s^T C_s e_s + \xi_s^T [e_s + \Theta_s + \Delta_s - \tau_s - \tau_e] \end{aligned} \tag{16}$$

where $\zeta_s = P_s(\ddot{q}_{\mathrm{sr}} + \Lambda_s \dot{e}_s + \lambda_s \beta(\dot{e}_s)), \Theta_s = Q_s \xi_s + Q_s \dot{q}_s + G_s + \zeta_s - \Pi_s$. By employing the RBFNN to approximate Θ_s, one has $\Theta_s = W_s^T \Psi_s + \epsilon_s$. The slave equivalent control input can be designed as

$$\tau_{\mathrm{seqv}} = e_s + \widehat{W}_s^T \Psi_s - \tau_e \tag{17}$$

The slave switching controller is given by

$$\tau_{\mathrm{sr}} = K_s \xi_s + (\widehat{\alpha}_{s0} + \widehat{\alpha}_{s1} |e_s| + \widehat{\alpha}_{s2} |\dot{e}_s|)\, sign(\xi_s) \tag{18}$$

where $\widehat{\alpha}_{\mathrm{si}}$ are the estimates of $\widehat{\alpha}_{\mathrm{si}} i = 0, 1, 2$. The total slave control law can be designed as follows

$$\begin{aligned} \tau_s &= \tau_{\mathrm{seqv}} + \tau_{\mathrm{sr}} \\ &= e_s + \widehat{W}_s^T \Psi_s - \tau_e + K_s \xi_s + (\widehat{\alpha}_{s0} + \widehat{\alpha}_{s1} |e_s| + \widehat{\alpha}_{s2} |\dot{e}_s|)\, sign(\xi_s) \end{aligned} \tag{19}$$

The parameters are updated by the following adaptive laws

$$\dot{\widehat{W}}_s = \gamma_s \Psi_s \xi_s^T - \mu \gamma_s \widehat{W}_s \tag{20}$$

$$\dot{\widehat{\alpha}}_{s0} = \varrho_{s0} \cdot |\xi_s| - \mu \varrho_{s0} \widehat{\alpha}_{s0} \tag{21}$$

$$\dot{\widehat{\alpha}}_{s1} = \varrho_{s1} \cdot |e_s| \cdot |\xi_s| - \mu \varrho_{s1} \widehat{\alpha}_{s1} \tag{22}$$

$$\dot{\widehat{\alpha}}_{s2} = \varrho_{s2} \cdot |\dot{e}_s| \cdot |\xi_s| - \mu \varrho_{s2} \widehat{\alpha}_{s2} \tag{23}$$

where $\gamma_s > 0, \mu > 0, \varrho_{\mathrm{si}} > 0$ ($i = 0, 1, 2$) are constants.

Theorem 1: Consider the slave system (1) and the surface (9), if the control law is set as (19) with adaptive laws (20)-(23), the closed-loop slave plant is bounded.

Proof 1: Consider the following candidate Lyapunov function

$$V_s = V_{s2}+\frac{1}{2}\widetilde{W}_s^T\gamma_s^{-1}\widetilde{W}_s+\frac{\widetilde{\alpha}_{s0}^2}{2\varrho_{s0}}+\frac{\widetilde{\alpha}_{s1}^2}{2\varrho_{s1}}+\frac{\widetilde{\alpha}_{s2}^2}{2\varrho_{s2}} \tag{24}$$

where $\widetilde{W}_s = W_s - \widehat{W}_s, \widetilde{\alpha}_{\text{si}} = \alpha_{\text{si}} - \widehat{\alpha}_{\text{si}} i = (0,1,2)$. The time-derivative of V_s gives

$$\begin{aligned}\dot{V}_s \quad &= -e_s^T C_s e_s + \xi_s^T\left[e_s + W_s^T\Psi_s + \epsilon_s + \Delta_s - \tau_s - \tau_e\right] \\ &\quad -\dot{\widehat{W}}_s\gamma_s^{-1}\widetilde{W}_s - \frac{\dot{\widehat{\alpha}}_{s0}\widetilde{\alpha}_{s0}^2}{\varrho_{s0}} - \frac{\dot{\widehat{\alpha}}_{s1}\widetilde{\alpha}_{s1}^2}{\varrho_{s1}} - \frac{\dot{\widehat{\alpha}}_{s2}\widetilde{\alpha}_{s2}^2}{\varrho_{s2}}\end{aligned} \tag{25}$$

Substituting the control law (19) into (25) yields

$$\begin{aligned}\dot{V}_s \quad &= -e_s^T C_s e_s - \xi_s^T K_s\xi_s + \widetilde{W}_s^T\Psi_s\xi_s \\ &+ \left[\xi_s^T\left(\epsilon_s + \Delta_s\right) - \left(\widehat{\alpha}_{s0} + \widehat{\alpha}_{s1}\left|e_s\right| + \widehat{\alpha}_{s2}\left|\dot{e}_s\right|\right)\left|\xi_s\right|\right] \\ &-\dot{\widehat{W}}_s\gamma_s^{-1}\widetilde{W}_s - \frac{\dot{\widehat{\alpha}}_{s0}\widetilde{\alpha}_{s0}^2}{\varrho_{s0}} - \frac{\dot{\widehat{\alpha}}_{s1}\widetilde{\alpha}_{s1}^2}{\varrho_{s1}} - \frac{\dot{\widehat{\alpha}}_{s2}\widetilde{\alpha}_{s2}^2}{\varrho_{s2}}\end{aligned} \tag{26}$$

Using $\widehat{\alpha}_{\text{si}} = \alpha_{\text{si}} - \widetilde{\alpha}_{\text{si}}, (i = 0,1,2)$, we get

$$\begin{aligned}\dot{V}_s \quad &= -e_s^T C_s e_s - \xi_s^T K_s\xi_s \\ &+ \left[\xi_s^T\left(\epsilon_s + D_s\right) - \left(\alpha_{s0} + \alpha_{s1}\left|e_s\right| + \alpha_{s2}\left|\dot{e}_s\right|\right)\left|\xi_s\right|\right] \\ &+\widetilde{W}_s^T\left[\Psi_s\xi_s^T - \gamma_s^{-1}\dot{\widehat{W}}_s\right] + \widetilde{\alpha}_{s0}\left[\left|\xi_s\right| - \frac{\dot{\widehat{\alpha}}_{s0}}{\varrho_{s1}}\right] \\ &+\widetilde{\alpha}_{s1}\left[\left|e_s\right|\left|\xi_s\right| - \frac{\dot{\widehat{\alpha}}_{s1}}{\varrho_{s1}}\right] + \widetilde{\alpha}_{s2}\left[\left|\dot{e}_s\right|\left|\xi_s\right| - \frac{\dot{\widehat{\alpha}}_{s2}}{\varrho_{s2}}\right]\end{aligned} \tag{27}$$

From Assumption 1 and (20)-(23), we have

$$\begin{aligned}\dot{V}_s \quad &\leq -\parallel C_s \parallel \parallel e_s^T \parallel - \parallel K_s \parallel \parallel \xi_s \parallel + \mu \parallel \widetilde{W}_s \parallel \parallel \widehat{W}_s \parallel \\ &\quad + \mu\widetilde{\alpha}_{s0}\widehat{\alpha}_{s0} + \mu\widetilde{\alpha}_{s1}\widehat{\alpha}_{s1} + \mu\widetilde{\alpha}_{s2}\widehat{\alpha}_{s2}\end{aligned} \tag{28}$$

By using the following inequalities

$$\begin{aligned}\parallel \widetilde{W}_s \parallel \parallel \widehat{W}_s \parallel \quad &\leq \frac{\|W_s\|^2}{2} - \frac{\|\widetilde{W}_s\|^2}{2} \\ \widetilde{\alpha}_{\text{si}}\widehat{\alpha}_{\text{si}} \quad &\leq \frac{\alpha_{\text{si}}^2}{2} - \frac{\widetilde{\alpha}_{\text{si}}^2}{2}, \ (i = 0,1,2)\end{aligned}$$

Equation (28) can be expressed as

$$\dot{V}_s \leq -b_{s1}V_s + b_{s2} \tag{29}$$

where $b_{s1} = min\left(2 \parallel C \parallel, 2 \parallel K_s \parallel, \mu\alpha_{s0}, \mu\alpha_{s1}, \mu\alpha_{s2}\right), b_{s2} = \frac{\|W_s\|^2}{2} + \frac{\alpha_{s0}^2}{2} + \frac{\alpha_{\text{si}}^2}{2}\frac{\alpha_{s2}^2}{2}$. Integrating the equation above yields

$$V_s \leq \frac{b_{s2}}{b_{s1}} + \left(V_s(0) - \frac{b_{s2}}{b_{s1}}\right)e^{-b_{s1}t} \tag{30}$$

When $t \longrightarrow \infty, V_s \leq \frac{b_{s2}}{b_{s1}}$. Therefore, all the error signals in the closed loop system are uniformly bounded in the compact set given by

$$\Phi_s = \left\{e_s, \xi_s, \widetilde{W}_s, \widetilde{\alpha}_{\text{si}}, (i = 0,1,2) : V_s \leq \frac{b_{s2}}{b_{s1}}\right\} \tag{31}$$

3.3. **Master control design.** A good reference impedance model is designed in the master side to generate the reference trajectory q_{mr} expressed as

$$\begin{aligned}&P_r\left(q_{\text{mr}}\right)\ddot{q}_{mr} + Q_r\left(q_{\text{mr}}, \dot{q}_{mr}\right)\dot{q}_{mr} + G_r\left(q_{\text{mr}}\right) \\ &\quad = \tau_h - \tau_e(t - d(t))\end{aligned} \tag{32}$$

where P_r, Q_r and G_r are positive definite diagonal matrices of the impedance model, $\tau(t-d(t))$ is the delayed environmental torque transmitted from the slave plant to the master via the communication channel. A controller τ_m is developed to have $q_m \longrightarrow q_{\text{mr}}$. Therefore, the tracking error between q_m and q_{mr} is

$$\begin{cases} e_m \quad = q_{\text{mr}} - q_m \\ \dot{e}_m \quad = \dot{q}_{mr} - \dot{q}_m \\ \ddot{e}_m \quad = \ddot{q}_{mr} + P_m^{-1}\left[Q_m\dot{q}_m + G_m + D_m - \Pi_m \right. \\ \qquad\qquad \left. -\tau_m - \tau_h\right] \end{cases} \tag{33}$$

The NFTSMC manifold is defined as [51]

$$\xi_m = \dot{e}_m + \Lambda_m e_m + \lambda_m\beta_m\left(e_m\right) \tag{34}$$

with$\beta_m\left(e_m\right)$ and its first time-derivative $\dot{\beta}_m\left(e_m\right)$ defined as

$$\beta_m(e_{mi}) = \begin{cases} \operatorname{sig}(e_{\mathrm{mi}})^{\sigma_{\mathrm{mi}}}, \ \bar{\xi}_{\mathrm{mi}} = 0 \ or \\ \qquad \bar{\xi}_{\mathrm{mi}} \neq 0, |e_{\mathrm{mi}}| > \varepsilon \\ \rho_{\mathrm{mi}} \ e_{\mathrm{mi}} + \ \eta_{\mathrm{mi}} \operatorname{sig}(e_{\mathrm{mi}})^{\omega_{\mathrm{mi}}}, \\ \qquad \bar{\xi}_{\mathrm{mi}} \neq 0, |e_{\mathrm{mi}}| \leq \varepsilon \end{cases}$$

$$\dot{\beta}_m(e_{\mathrm{mi}}) = \begin{cases} \sigma_{\mathrm{mi}} |e_{\mathrm{mi}}|^{\sigma_{\mathrm{mi}-1}} \dot{e_{\mathrm{mi}}}, \ \bar{\xi}_{\mathrm{mi}} = 0 \ or \\ \qquad (\bar{\xi}_{\mathrm{mi}} \neq 0, |e_{\mathrm{mi}}| > \varepsilon) \\ \rho_{\mathrm{mi}} \ \dot{e_{\mathrm{mi}}} + \ \eta_{\mathrm{mi}} \omega_{\mathrm{mi}} |e_{\mathrm{mi}}|^{\ \omega_{\mathrm{mi}}-1} \ \dot{e_{\mathrm{mi}}}, \\ \qquad \bar{\xi}_{\mathrm{mi}} \neq 0, |e_{\mathrm{mi}}| \leq \varepsilon \\ \qquad i = 1, 2, \ldots, n \end{cases} \tag{35}$$

where $\bar{\xi}_{\mathrm{mi}} = \dot{e}_{\mathrm{mi}} + \Lambda_{\mathrm{mi}} e_{\mathrm{mi}} + \lambda_{\mathrm{mi}} \beta_{\mathrm{mi}}(e_{\mathrm{mi}}), 0 < \sigma_{\mathrm{mi}} < 1, 1 < \omega_{\mathrm{mi}} < 2, \varepsilon > 0$, and ρ_{mi} and η_{mi} meet the following conditions

$$\begin{aligned} \rho_{\mathrm{mi}} &= [(\omega_{\mathrm{mi}} - \sigma_{\mathrm{mi}}) / (\omega_{\mathrm{mi}} - 1)] \, \varepsilon^{\sigma_{\mathrm{si}}-1} \\ \eta_{\mathrm{mi}} &= [(\sigma_{\mathrm{mi}} - 1) / (\omega_{\mathrm{mi}} - 1)] \, \varepsilon^{\sigma_{\mathrm{mi}}-\omega_{\mathrm{mi}}} \end{aligned}$$

Define the Lyapunov function V_{m1} as

$$V_{m1} = \frac{1}{2} e_m^T e_m \tag{36}$$

The derivative of V_{m1} with respect to time can be computed as

$$\dot{V}_{m1} = e_m^T [\dot{q}_{\mathrm{mr}} - \dot{q}_m] \tag{37}$$

The virtual control input is expressed as

$$\dot{q}_m = -\xi_m + \dot{q}_{\mathrm{mr}} + C_m e_m \tag{38}$$

where $C_m = C_m^T > 0$ is a constant diagonal matrix. Inserting the controller (38) into (37) gives

$$\dot{V}_{m1} = -e_m^T C_m e_m + e_m^T \xi_m \tag{39}$$

Then, consider the Lyapunov function

$$V_{m2} = \frac{1}{2} e_m^T e_m + \frac{1}{2} \xi_m^T P_m \xi_m \tag{40}$$

The time derivative of V_{m2} can be derived as

$$\begin{aligned} \dot{V}_{m2} &= -e_m^T C_m e_m + e_m^T \xi_m + \frac{1}{2} \xi_m^T \dot{P}_m \xi_m + \dot{\xi}_m^T P_m \xi_m \\ &= -e_m^T C_m e_m + e_m^T \xi_m + \xi_m^T \dot{P}_m \xi_m \\ &\quad + \xi_m^T [Q_m \dot{q}_m + G_m + \Delta_m + \zeta_m - \Pi_m - \tau_m - \tau_h] \\ &= -e_m^T C_m e_m + \frac{1}{2} \xi_m^T \left[\dot{P}_m - 2Q_m \right] \xi_m \\ &\quad + \xi_m^T [e_m + Q_m \xi_m + Q_m \dot{q}_m + G_m \\ &\quad + \Delta_m + \zeta_m - \Pi_m - \tau_m - \tau_h] \\ &= -e_m^T C_m e_m + \xi_m^T [e_m + \Theta_m + \Delta_m \\ &\quad - \tau_m - \tau_h] \end{aligned} \tag{41}$$

where $\zeta_m = P_m \left(\ddot{q}_{\mathrm{mr}} + \Lambda_m \dot{e}_m + \lambda_m \dot{\beta}(e_m) \right), \Theta_m = Q_m \xi_m + Q_m \dot{q}_m + G_m + \zeta_m - \Pi_m$. By utilizing the RBFNN, we can have $\Theta_m = W_m^T \Psi_m + \epsilon_m$. Then, the master equivalent control law τ_{meqv} is derived as

$$\tau_{\mathrm{meqv}} = e_m + \widehat{W}_m^T \Psi_m - \tau_h \tag{42}$$

The adaptive master switching controller is given by

$$\tau_{\mathrm{mr}} = K_m \xi_m + (\widehat{\alpha}_{m0} + \widehat{\alpha}_{m1} |e_m| + \widehat{\alpha}_{m2} |\dot{e}_m|) \, sign(\xi_m) \tag{43}$$

where $\widehat{\alpha}_{\mathrm{mi}}$ are the estimates of $\widehat{\alpha}_{\mathrm{mi}} i = 0, 1, 2$. Thus, the overall master control law is designed as

$$\begin{aligned}\tau_m &= \tau_{\text{meqv}} + \tau_{\text{mr}} \\ &= e_m + \widehat{W}_m^T \Psi_m - \tau_e + K_m \xi_m \\ &+ \left(\widehat{\alpha}_{m0} + \widehat{\alpha}_{m1} \left|e_m\right| + \widehat{\alpha}_{m2} \left|\dot{e}_m\right|\right) sign\left(\xi_m\right)\end{aligned} \tag{44}$$

The parameters are updated by the following adaptive laws

$$\dot{\widehat{W}}_m = \gamma_m \Psi_m \xi_m^T - \mu \gamma_m \widehat{W}_m \tag{45}$$

$$\dot{\widehat{\alpha}}_{m0} = \varrho_{m0} \cdot \left|\xi_m\right| - \mu \varrho_{m0} \widehat{\alpha}_{m0} \tag{46}$$

$$\dot{\widehat{\alpha}}_{m1} = \varrho_{m1} \cdot \left|e_m\right| \cdot \left|\xi_m\right| - \mu \varrho_{m1} \widehat{\alpha}_{m1} \tag{47}$$

$$\dot{\widehat{\alpha}}_{m2} = \varrho_{m2} \cdot \left|\dot{e}_m\right| \cdot \left|\xi_m\right| - \mu \varrho_{m2} \widehat{\alpha}_{m2} \tag{48}$$

where $\gamma_m > 0, \mu > 0 \varrho_{\text{mi}} > 0$ ($i = 0, 1, 2$) are constants.

Theorem 2: Consider the master system (2) and the surface (34), if the control law is set as (44) with adaptive laws (45)-(48), the closed-loop master system is bounded.

Proof 2: Consider the following Lyapunov function

$$V_m = V_{m2} + \frac{1}{2} \widetilde{W}_m^T \gamma_m^{-1} \widetilde{W}_m + \frac{\widetilde{\alpha}_{m0}^2}{2\varrho_{m0}} + \frac{\widetilde{\alpha}_{m1}^2}{2\varrho_{m1}} + \frac{\widetilde{\alpha}_{m2}^2}{2\varrho_{m2}} \tag{49}$$

where $\widetilde{W}_m = W_m - \widehat{W}_m, \widetilde{\alpha}_{\text{mi}} = \alpha_{\text{mi}} - \widehat{\alpha}_{\text{mi}} i = (0, 1, 2)$. The derivative of V_m with respect to time can be derived as

$$\begin{aligned}\dot{V}_m &= -e_m^T C_m e_m + \xi_m^T \left[e_m + W_m^T \Psi_m + \epsilon_m \right. \\ &\left. + \Delta_m - \tau_m - \tau_e\right] - \dot{\widehat{W}}_m \gamma_m^{-1} \widetilde{W}_m - \frac{\dot{\widehat{\alpha}}_{m0} \widetilde{\alpha}_{m0}^2}{\varrho_{m0}} \\ &- \frac{\dot{\widehat{\alpha}}_{m1} \widetilde{\alpha}_{m1}^2}{\varrho_{m1}} - \frac{\dot{\widehat{\alpha}}_{m2} \widetilde{\alpha}_{m2}^2}{\varrho_{m2}}\end{aligned} \tag{50}$$

Substituting the control law (44) into (50) yields

$$\begin{aligned}\dot{V}_m &= -e_m^T C_m e_m - \xi_m^T K_m \xi_m + \widetilde{W}_m^T \Psi_m \xi_m \\ &+ \left[\xi_m^T \left(\epsilon_m + \Delta_m\right) - \left(\widehat{\alpha}_{m0} + \widehat{\alpha}_{m1} \left|e_m\right| + \widehat{\alpha}_{m2} \left|\dot{e}_m\right|\right) \left|\xi_m\right|\right] \\ &- \dot{\widehat{W}}_m \gamma_m^{-1} \widetilde{W}_m - \frac{\dot{\alpha}_{m0} \widetilde{\alpha}_{m0}^2}{\varrho_{m0}} - \frac{\dot{\widehat{\alpha}}_{m1} \widetilde{\alpha}_{m1}^2}{\varrho_{m1}} - \frac{\dot{\widehat{\alpha}}_{m2} \widetilde{\alpha}_{m2}^2}{\varrho_{m2}}\end{aligned} \tag{51}$$

Using $\widehat{\alpha}_{\text{mi}} = \alpha_{\text{mi}} - \widetilde{\alpha}_{\text{mi}}$, $(i = 0, 1, 2)$, we have

$$\begin{aligned}\dot{V}_m &= -e_m^T C_m e_m - \xi_m^T K_m \xi_m \\ &+ \left[\xi_m^T \left(\epsilon_m + \Delta_m\right) - \left(\alpha_{m0} + \alpha_{m1} \left|e_m\right| + \alpha_{m2} \left|\dot{e}_m\right|\right) \left|\xi_m\right|\right] \\ &+ \widetilde{W}_m^T \left[\Psi_m \xi_m^T - \gamma_m^{-1} \dot{\widehat{W}}_m\right] + \widetilde{\alpha}_{m0} \left[\left|\xi_m\right| - \frac{\dot{\widehat{\alpha}}_{m0}}{\varrho_{m0}}\right] \\ &+ \widetilde{\alpha}_{m1} \left[\left|e_m \| \xi_m\right| - \frac{\dot{\widehat{\alpha}}_{m1}}{\varrho_{m1}}\right] + \widetilde{\alpha}_{m2} \left[\left|\dot{e}_m\right| \left|\xi_m\right| - \frac{\dot{\widehat{\alpha}}_{m2}}{\varrho_{m2}}\right]\end{aligned} \tag{52}$$

By substituting (45)-(48) into (52), we have

$$\begin{aligned}\dot{V}_m &\leq - \| C_m \| \| e_m^T \| - \| K_m \| \| \xi_m \| + \mu \| \widetilde{W}_m \| \| \widehat{W}_m \| \\ &+ \mu \widetilde{\alpha}_{m0} \widehat{\alpha}_{m0} + \mu \widetilde{\alpha}_{m1} \widehat{\alpha}_{m1} + \mu \widetilde{\alpha}_{m2} \widehat{\alpha}_{m2}\end{aligned} \tag{53}$$

The following inequalities hold

$$\begin{aligned}\| \widetilde{W}_m \| \| \widehat{W}_m \| &\leq \frac{\|W_m\|^2}{2} - \frac{\|\widetilde{W}_m\|^2}{2} \\ \widetilde{\alpha}_{\text{mi}} \widehat{\alpha}_{\text{mi}} &\leq \frac{\alpha_{\text{mi}}^2}{2} - \frac{\widetilde{\alpha}_{\text{mi}}^2}{2}, \ (i = 0, 1, 2)\end{aligned}$$

Equation (53) can be expressed as

$$\dot{V}_m \leq -b_{m1} V_m + b_{m2} \tag{54}$$

where $b_{m1} = min\left(2 \| C_m \|, 2 \| K_m \|, \mu \alpha_{m0}, \mu \alpha_{m1}, \mu \alpha_{m2}\right), b_{m2} = \mu \frac{\alpha_{m0}^2}{2} + \mu \frac{\alpha_{m1}^2}{2} + \mu \frac{\alpha_{m2}^2}{2}$. By computing the general solution of (54), one has

$$V_m \leq \frac{b_{m2}}{b_{m1}} + \left(V_m(0) - \frac{b_{m2}}{b_{m1}}\right) e^{-b_{m1} t} \tag{55}$$

When $t \longrightarrow \infty, V_m \leq \frac{b_{m2}}{b_{m1}}$. Therefore, all the error signals in the closed loop system are uniformly bounded in the compact set expressed as

$$\Phi_m = \left\{e_m, \xi_m, \widetilde{W}_m, \widetilde{\alpha}_{\text{mi}}, (i = 0, 1, 2) : V_m \leq \frac{b_{m2}}{b_{m1}}\right\} \tag{56}$$

Remark 1: Our work cannot be compared with that of [41]. This is because we take into account the time-varying delays in the communication channel, and the actuator deadzone in both master and slave plants.

4. COMPUTER SIMULATION

This section presents the simulation results of the 2-degree of freedom teleoperation system under the action of the BNFTSMC-RBFNN. The dynamic descriptions and parameters of the teleoperation system are given in [30]. The time-varying delay in the communication channel is set as $d(t) = 0.2 + 0.02sin(4t) + 0.05cos(7t)$. The initial conditions of the system are $q_i(0) = \dot{q}_i(0) = \begin{bmatrix} 0.1 & 0.1 \end{bmatrix}^T$ (i=m,s). The external disturbances are chosen as $\Delta_i = [0.5sin(2)0.5sin(2)]^T(i = m, s)$. The human force to drive the two joints is $\tau_h = [5cos(t)5cos(t)]^T$. When the slave manipulator is in contact with the environment, the contact force is modelled as a passive spring force expressed as

$$\tau_e = \begin{cases} p_e\left(q_s - q_e\right) & q_s \geq q_e \\ 0 & q_s < q_e \end{cases} \tag{57}$$

where $p_e = 1\ N/m$ denote the stiffness constant of the object to be grasped, $q_e = 1.5\ m$ stand for the contact position of the slave with the environment.

The parameters of the reference trajectories are set as $P_r = diag\begin{bmatrix} 1 & 1 \end{bmatrix}, Q_r = diag\begin{bmatrix} 0 & 0 \end{bmatrix}, G_r = diag\begin{bmatrix} 4 & 4 \end{bmatrix} q_{\mathrm{mr}}$. The low pass filter for generating the slave reference trajectories is designed as $\tau_f = 0.002$. The parameters of the controllers are: $\Lambda_s = diag[9090], \Lambda_m = diag\begin{bmatrix} 100 & 100 \end{bmatrix}, \lambda_s = diag\begin{bmatrix} 1 & 1 \end{bmatrix}, \lambda_m = diag\begin{bmatrix} 1 & 1 \end{bmatrix}, K_s = diag\begin{bmatrix} 19 & 19 \end{bmatrix}, K_m = diag[2223]$, the initial conditions of the update laws are $\varrho_{\mathrm{si}}(0) = \varrho_{\mathrm{mi}}(0) = 0.01(i = 0, 1, 2)$. The number of RBFNN node is $5, v = 2$, $\gamma_s = \gamma_m = 0.05, \mu = 0.0001, c = \begin{bmatrix} -4 & -2 & 0 & 1 \end{bmatrix}$.

The position tracking results of the master and slave plants are depicted in Fig. 2 and Fig. 3 respectively. The trajectory tracking deviations are very small (of order 10^{-5}) as shown in Fig. 4 and Fig. 5. Therefore, a good tracking performance is achieved. The responses of the input torques of the master and the slave are displayed in Fig. 6, and Fig. 7, respectively. Moreover, it can be observed that the slave's control torque is faster than the master's control torque. This is due to the fact that the slave's control torque puts in more effort to follow the delayed information from the master plant.

5. CONCLUSION

In this article, a BNFTSMC-RBFNN has been designed for uncertain bilateral teleoperation systems with time-varying delays and unknown actuator dead-zone. The devised scheme guarantees that the position tracking errors asymptotically converge to a very small neighborhood of zero. The BNFTSMC-RBFNN is model free and the dead-zone inverse and its prior knowledge are not needed. As such, the proposed control technique is easy to be implemented in physical system. The effectiveness of the proposed controller has been verified via numerical simulations. Moreover, its effectiveness in practical application will be verified when the hardware of the teleoperation system is acquired.

6. ACKNOWLEDGMENTS

"The second author would like to thank the Deanship of Scientific Research (DSR) at KFUPM for support through distinguished professorship award project no. **DUP 19106**.

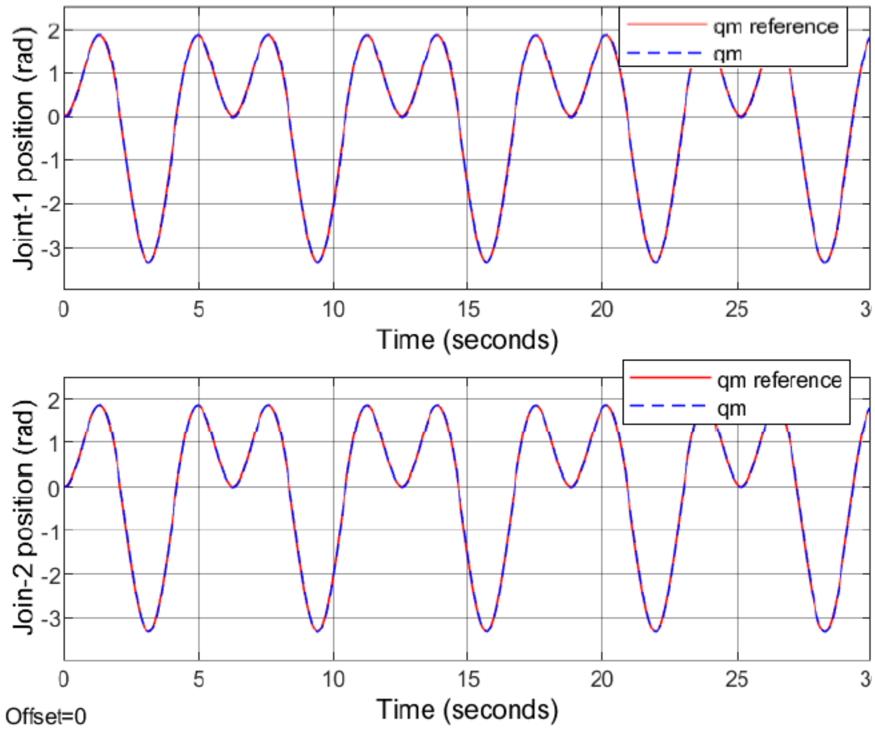

FIGURE 2. Position tracking result of the master plant

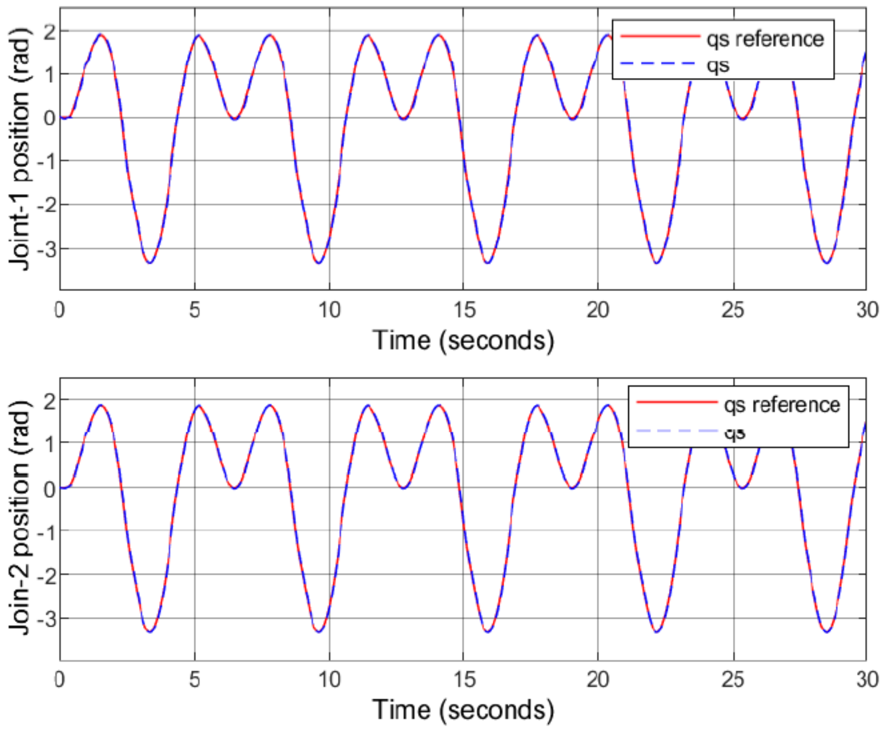

FIGURE 3. Position tracking result of the slave plant

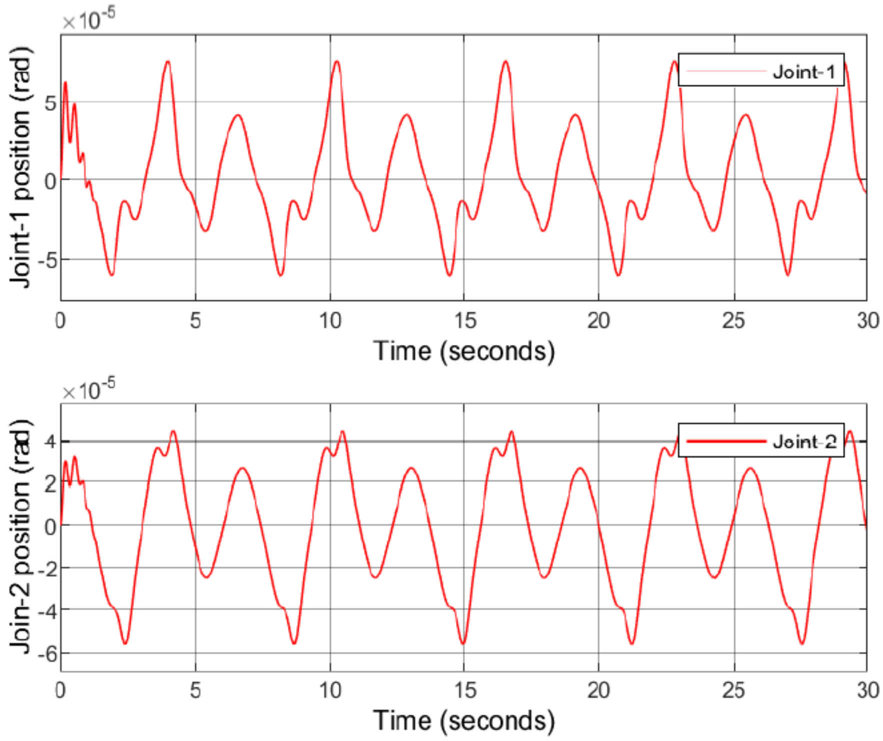

FIGURE 4. Position tracking error of the master plant

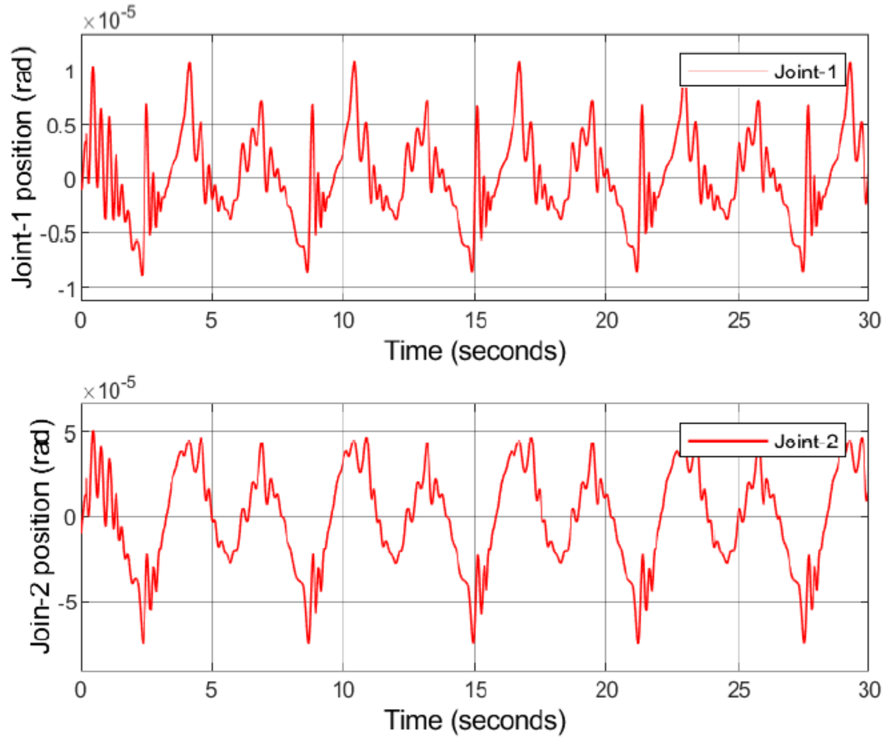

FIGURE 5. Position tracking error of the slave plant

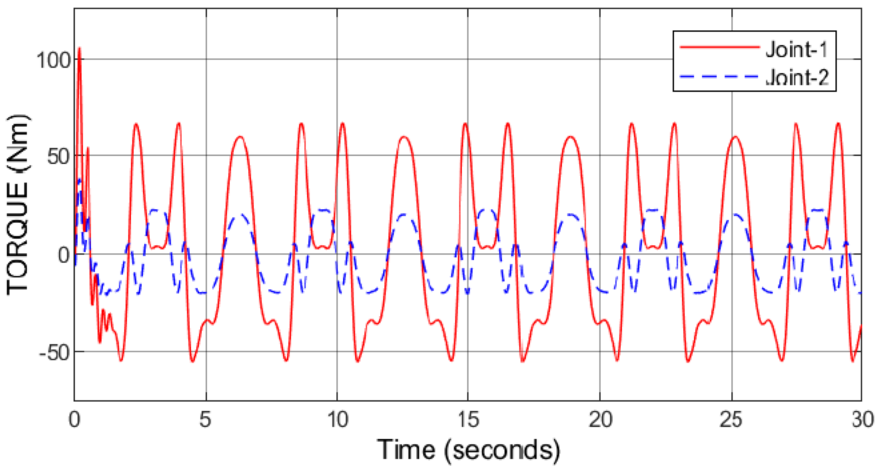

Figure 6. Input torque of the master plant

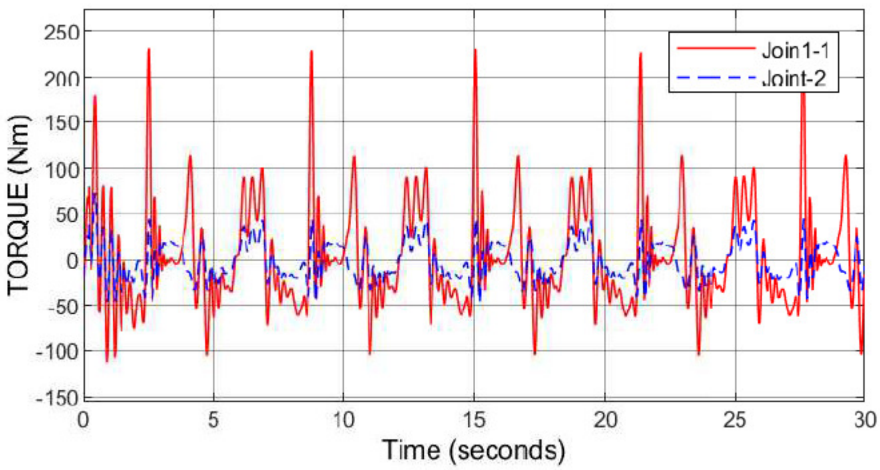

Figure 7. Input torque of the slave plant

References

[1] M.M. Hamdan, M.S. Mahmoud, Control of teleoperation systems in the presence of cyber attacks: A survey, Int. J. Robot. Autom. 10 (2021) 235. https://doi.org/10.11591/ijra.v10i3.pp235-260.

[2] F. Brizzi, L. Peppoloni, A. Graziano, E.D. Stefano, C.A. Avizzano, E. Ruffaldi, Effects of augmented reality on the performance of teleoperated industrial assembly tasks in a robotic embodiment, IEEE Trans. Human-Mach. Syst. 48 (2018) 197–206. https://doi.org/10.1109/THMS.2017.2782490.

[3] D. Sun, A. Kiselev, Q. Liao, T. Stoyanov, A. Loutfi, A new mixed-reality-based teleoperation system for telepresence and maneuverability enhancement, IEEE Trans. Human-Mach. Syst. 50 (2020) 55–67. https://doi.org/10.1109/THMS.2019.2960676.

[4] F. Azimifar, S. Ahmadkhosravi Rozi, A. Saleh, I. Afyouni, Transparency performance improvement for multi-master multi-slave teleoperation systems with external force estimation, Trans. Inst. Measure. Control. 40 (2018) 3851–3859. https://doi.org/10.1177/0142331217740178.

[5] D. Sun, Q. Liao, A. Loutfi, Single master bimanual teleoperation system with efficient regulation, IEEE Trans. Robot. 36 (2020) 1022–1037. https://doi.org/10.1109/TRO.2020.2973099.

[6] A.A. Ghavifekr, A.R. Ghiasi, M.A. Badamchizadeh, F. Hashemzadeh, Exponential stability of bilateral sampled-data teleoperation systems using multirate approach, ISA Trans. 105 (2020) 190–197. https://doi.org/10.1016/j.isatra.2020.05.044.

[7] R. Baranitha, R. Rakkiyappan, R. Mohajerpoor, S. Al-Wais, Stability analysis of nonlinear telerobotic systems with time-varying communication channel delays using general integral inequalities, Inform. Sci. 465 (2018) 353–372. https://doi.org/10.1016/j.ins.2018.07.014.

[8] H. Chen, P. Huang, Z. Liu, Z. Ma, Time delay prediction for space telerobot system with a modified sparse multivariate linear regression method, Acta Astronautica. 166 (2020) 330–341. https://doi.org/10.1016/j.actaastro.2019.10.027.

[9] C. Yang, X. Wang, L. Cheng, H. Ma, Neural-learning-based telerobot control with guaranteed performance, IEEE Trans. Cybern. 47 (2017) 3148–3159. https://doi.org/10.1109/TCYB.2016.2573837.

[10] C.P. Vo, X.D. To, K.K. Ahn, A novel force sensorless reflecting control for bilateral haptic teleoperation system, IEEE Access. 8 (2020) 96515–96527. https://doi.org/10.1109/ACCESS.2020.2994374.

[11] C. Yang, J. Luo, Y. Pan, Z. Liu, C.-Y. Su, Personalized variable gain control with tremor attenuation for robot teleoperation, IEEE Trans. Syst. Man Cybern, Syst. 48 (2018) 1759–1770. https://doi.org/10.1109/TSMC.2017.2694020.

[12] A. Javid, M. ali Nekoui, An adaptive controller for bilateral teleoperation systems with uncertain kinematics and dynamics, in: 2018 6th RSI International Conference on Robotics and Mechatronics (IcRoM), IEEE, Tehran, Iran, 2018: pp. 59–64. https://doi.org/10.1109/ICRoM.2018.8657549.

[13] Z. Wang, Y. Tian, Y. Sun, B. Liang, Finite-time output-feedback control for teleoperation systems subject to mismatched term and state constraints, J. Franklin Inst. 357 (2020) 11421–11447. https://doi.org/10.1016/j.jfranklin.2019.07.013.

[14] K.D. Kallu, S.J. Abbasi, H. Khan, J. Wang, M.C. Lee, Tele-operated bilateral control of hydraulic manipulator using a robust controller based on the sensorless estimated reaction force, Appl. Sci. 9 (2019) 1995. https://doi.org/10.3390/app9101995.

[15] S. Lampinen, J. Koivumaki, W.-H. Zhu, J. Mattila, Force-sensor-less bilateral teleoperation control of dissimilar master-slave system with arbitrary scaling, IEEE Trans. Contr. Syst. Technol. (2021) 1–15. https://doi.org/10.1109/TCST.2021.3091314.

[16] B. Aboutalebian, H.A. Talebi, S. Etedali, A.A. Suratgar, Adaptive control of teleoperation system based on nonlinear disturbance observer, Eur. J. Control. 53 (2020) 109–116. https://doi.org/10.1016/j.ejcon.2019.10.002.

[17] A. Mohammadi, H. Dallali, Disturbance observer applications in rehabilitation robotics: an overview, in: Powered Prostheses, Elsevier, 2020: pp. 113–133. https://doi.org/10.1016/B978-0-12-817450-0.00005-5.

[18] T. Wang, Y. Li, J. Zhang, Y. Zhang, A novel bilateral impedance controls for underwater tele-operation systems, Appl. Soft Comput. 91 (2020) 106194. https://doi.org/10.1016/j.asoc.2020.106194.

[19] S. Hu, Y. Liu, Event-triggered control for adaptive bilateral teleoperators with communication delays, IET Control Theory Appl. 14 (2020) 427–437. https://doi.org/10.1049/iet-cta.2019.0298.

[20] Y. Yang, C. Hua, J. Li, X. Guan, Finite-time output-feedback synchronization control for bilateral teleoperation system via neural networks, Information Sciences. 406–407 (2017) 216–233. https://doi.org/10.1016/j.ins.2017.04.034.

[21] P. Rasouli, A. Forouzantabar, M. Moattari, M. Azadi, Fault-tolerant control of teleoperation systems with flexible-link slave robot and disturbance compensation, Iran. J. Sci. Technol. Trans. Electr. Eng. 44 (2020) 1487–1499. https://doi.org/10.1007/s40998-020-00309-5.

[22] Y. Ji, D. Liu, Y. Guo, Adaptive neural network based position tracking control for Dual-master/Single-slave teleoperation system under communication constant time delays, ISA Trans. 93 (2019) 80–92. https://doi.org/10.1016/j.isatra.2019.03.019.

[23] H. Khan, S.J. Abbasi, M.C. Lee, DPSO and inverse Jacobian-based real-time inverse kinematics with trajectory tracking using integral SMC for teleoperation, IEEE Access. 8 (2020) 159622–159638. https://doi.org/10.1109/ACCESS.2020.3020318.

[24] Z. Wang, Z. Chen, B. Liang, B. Zhang, A novel adaptive finite time controller for bilateral teleoperation system, Acta Astronautica. 144 (2018) 263–270. https://doi.org/10.1016/j.actaastro.2017.12.046.

[25] P.M. Kebria, A. Khosravi, S.M.J. Jalali, S. Nahavandi, Adaptive type-2 fuzzy control scheme for robust teleoperation under time-varying delay and uncertainties, in: 2019 IEEE 15th International Conference

on Automation Science and Engineering (CASE), IEEE, Vancouver, BC, Canada, 2019: pp. 1631–1636. https://doi.org/10.1109/COASE.2019.8843013.

[26] P.M. Kebria, A. Khosravi, S. Nahavandi, D. Wu, F. Bello, Adaptive type-2 fuzzy neural-network control for teleoperation systems with delay and uncertainties, IEEE Trans. Fuzzy Syst. 28 (2020) 2543–2554. https://doi.org/10.1109/TFUZZ.2019.2941173.

[27] R. Ebrahimi Bavili, A. Akbari, R. Mahboobi Esfanjani, Passivity-based control of nonlinear teleoperation systems with non-passive interaction forces, Intel. Serv. Robot. 13 (2020) 419–437. https://doi.org/10.1007/s11370-020-00327-6.

[28] P.M. Kebria, A. Khosravi, S. Nahavandi, D. Watters, G. Guest, P. Shi, Robust adaptive control of internet-based bilateral teleoperation systems with time-varying delay and model uncertainties, in: 2019 IEEE International Conference on Industrial Technology (ICIT), IEEE, Melbourne, Australia, 2019: pp. 187–192. https://doi.org/10.1109/ICIT.2019.8755182.

[29] Y. Li, K. Zhang, K. Liu, R. Johansson, Y. Yin, Neural-network-based adaptive control for bilateral teleoperation with multiple slaves under Round-Robin scheduling protocol, Int. J. Control. 94 (2021) 1461–1474. https://doi.org/10.1080/00207179.2019.1652853.

[30] Y. Li, Y. Yin, S. Zhang, J. Dong, R. Johansson, Composite adaptive control for bilateral teleoperation systems without persistency of excitation, J. Franklin Inst. 357 (2020) 773–795. https://doi.org/10.1016/j.jfranklin.2019.04.001.

[31] Z. Wang, Z. Chen, Y. Zhang, X. Yu, X. Wang, B. Liang, Adaptive finite-time control for bilateral teleoperation systems with jittering time delays, Int. J. Robust Nonlinear Control. 29 (2019) 1007–1030. https://doi.org/10.1002/rnc.4423.

[32] A. Zakerimanesh, F. Hashemzadeh, A. Torabi, M. Tavakoli, A cooperative paradigm for task-space control of multilateral nonlinear teleoperation with bounded inputs and time-varying delays, Mechatronics. 62 (2019) 102255. https://doi.org/10.1016/j.mechatronics.2019.102255.

[33] Z. Chen, F. Huang, C. Yang, B. Yao, Adaptive fuzzy backstepping control for stable nonlinear bilateral teleoperation manipulators with enhanced transparency performance, IEEE Trans. Ind. Electron. 67 (2020) 746–756. https://doi.org/10.1109/TIE.2019.2898587.

[34] P.M. Kebria, A. Khosravi, S. Nahavandi, P. Shi, R. Alizadehsani, Robust adaptive control scheme for teleoperation systems with delay and uncertainties, IEEE Trans. Cybern. 50 (2020) 3243–3253. https://doi.org/10.1109/TCYB.2019.2891656.

[35] Z. Chen, F. Huang, W. Sun, J. Gu, B. Yao, RBF-neural-network-based adaptive robust control for nonlinear bilateral teleoperation manipulators with uncertainty and time delay, IEEE/ASME Trans. Mechatron. 25 (2020) 906–918. https://doi.org/10.1109/TMECH.2019.2962081.

[36] J. Yan, X. Yang, X. Luo, X. Guan, Dynamic gain control of teleoperating cyber-physical system with time-varying delay, Nonlinear Dyn. 95 (2019) 3049–3062. https://doi.org/10.1007/s11071-018-04740-6.

[37] Z. Wang, B. Liang, Y. Sun, T. Zhang, Adaptive fault-tolerant prescribed-time control for teleoperation systems with position error constraints, IEEE Trans. Ind. Inf. 16 (2020) 4889–4899. https://doi.org/10.1109/TII.2019.2951329.

[38] Z. Zhao, C.K. Ahn, H.-X. Li, Dead zone compensation and adaptive vibration control of uncertain spatial flexible riser systems, IEEE/ASME Trans. Mechatron. 25 (2020) 1398–1408. https://doi.org/10.1109/TMECH.2020.2975567.

[39] C. Hua, Y. Wang, Y. Yang, X. Guan, Force feedback control for bilateral teleoperation system with unknown Prandtl-Ishlinskii hysteresis, J. Franklin Inst. 357 (2020) 8321–8341. https://doi.org/10.1016/j.jfranklin.2020.03.001.

[40] H. Wang, P.X. Liu, S. Liu, Adaptive neural synchronization control for bilateral teleoperation systems with time delay and backlash-like hysteresis, IEEE Trans. Cybern. 47 (2017) 3018–3026. https://doi.org/10.1109/TCYB.2016.2644656.

[41] X. Liu, M. Tavakoli, Bilateral adaptive control of nonlinear teleoperation systems with uncertain dynamics and dead-zone, J. Dyn. Syst. Measure. Control. 140 (2018) 121004. https://doi.org/10.1115/1.4040666.

[42] H. Zhang, A. Song, H. Li, S. Shen, Novel adaptive finite-time control of teleoperation system with time-varying delays and input saturation, IEEE Trans. Cybern. 51 (2021) 3724–3737. https://doi.org/10.1109/TCYB.2019.2924446.

[43] L. Zhao, L. Liu, Y. Wang, H. Yang, Active disturbance rejection control for teleoperation systems with actuator saturation, Asian J. Control. 21 (2019) 702–713. https://doi.org/10.1002/asjc.1767.

[44] A. Zakerimanesh, F. Hashemzadeh, M. Tavakoli, Task-space synchronisation of nonlinear teleoperation with time-varying delays and actuator saturation, Int. J. Control. 93 (2020) 1328–1344. https://doi.org/10.1080/00207179.2018.1506158.

[45] X. Yang, J. Yan, C. Hua, X. Guan, Effects of quantization and saturation on performance in bilateral teleoperator, Int J Robust Nonlinear Control. 30 (2020) 121–141. https://doi.org/10.1002/rnc.4751.

[46] L. Mohammadi, A. Alfi, Guaranteed cost control in delayed teleoperation systems under actuator saturation, Iran. J. Sci. Technol. Trans. Electr. Eng. 43 (2019) 827–835. https://doi.org/10.1007/s40998-019-00206-6.

[47] P. Rasouli, A. Forouzantabar, M. Moattari, M. Azadi, Disturbance observer-based control of master and slave systems with input saturation, Aut. Control Comp. Sci. 54 (2020) 19–29. https://doi.org/10.3103/S0146411620010095.

[48] Y. Gong, B. Wu, Y. Ji, Synchronization analysis of bilateral teleoperation system with quantization and saturation, in: 2020 39th Chinese Control Conference (CCC), IEEE, Shenyang, China, 2020: pp. 4604–4609. https://doi.org/10.23919/CCC50068.2020.9188389.

[49] Y. Yang, J. Li, C. Hua, X. Guan, Adaptive synchronization control design for flexible telerobotics with actuator fault and input saturation: Adaptive synchronization control design for flexible telerobotics with actuator fault and input saturation, Int. J. Robust. Nonlinear Control. 28 (2018) 1016–1034. https://doi.org/10.1002/rnc.3922.

[50] B. Xu, Composite learning finite-time control with application to quadrotors, IEEE Trans. Syst. Man Cybern, Syst. 48 (2018) 1806–1815. https://doi.org/10.1109/TSMC.2017.2698473.

[51] Y. Wang, L. Liu, J. Chen, F. Ju, B. Chen, H. Wu, Practical robust control of cable-driven robots with feedforward compensation, Advances in Engineering Software. 145 (2020) 102801. https://doi.org/10.1016/j.advengsoft.2020.102801.